Construction and Building Materials 93 (2015) 498–505

Contents lists available at ScienceDirect

Construction and Building Materials

journal homepage: www.elsevier.com/locate/conbuildmat

Flexural strengths and fibre efficiency of steel-fibre-reinforced, roller-compacted, polymer modified concrete

John N. Karadelis *, Yougui Lin

Department of Civil Engineering, Architecture and Building, Faculty of Engineering and Computing, Coventry University, Coventry, W. Midlands, CV1 5FB, UK

HIGHLIGHTS

- Standard equivalent flexural strengths are established for overlay pavement design.
- SBRPMC1.5%-35 mix is optimal for flexural and bond strengths and workability.
- Lower w/c is the main reason for superior performance of fibre in the SFR–RC–PMC.
- The fibre bridging law can be an index of fibre efficiency in a mix design.
- The fibre bridging law can be used to predict the flexural performance of beams.

ARTICLE INFO

Article history:
Received 25 July 2014
Received in revised form 30 March 2015
Accepted 9 April 2015

Keywords:
Steel fibre-reinforced
Roller-compacted
Polymer-modified
Concrete
Fibre efficiency

ABSTRACT

A new material suitable for the structural repair of concrete pavements has been developed at Coventry University exhibiting high flexural, shear and bond strengths and high resistance to reflection cracking, demonstrating also unique *placeability* and *compactability* properties.

This article deals with the *standard* equivalent flexural strengths evaluated using the *identical fibre bridging concept* and the size effect. Correlation of flexural strengths for beams of different sizes was achieved and the efficiency of fibre in the mix was scrutinised. It was concluded that the efficiency was much higher in the new steel-fibre reinforced, roller compacted, polymer modified concrete (SFR–RC–PMC) mix than in conventional concrete. The high efficiency revealed by the fibre bridging law is mainly attributed to a lower water to cement ratio. It was also found that the fibre aspect ratio influences significantly the flexural performance of the new material. The very high flexural strength extracted from the SFR–RC–PMC, compared to conventional steel-fibre reinforced concrete is very favourable to worn concrete pavement rehabilitation.

1. Introduction

Part of the 'Green Overlays' research lead by the authors for the last four years involved the development of special concrete mixes used as overlay material, fully bonded on worn concrete pavements. This material exhibits high flexural, shear and bond strengths and high resistance to reflection cracking. It also demonstrates unique *placeability* and *compactability* properties, hence it can be placed on the damaged surface by an asphalt paver and compacted by a vibrating roller [1]. The mixes were named steel-fibre-reinforced, roller-compacted, polymer modified concrete (SFR–RC–PMC). The steel fibre in the mix retards and contains reflective cracking, the polymers enhance its strength and achieve good bond with the old concrete and the roller compaction ensures quick construction. These types of mixes were different from conventional roller-compacted concrete (RCC). Specifically, the optimal water content of the former determined by the modified-light (M-L) compaction method proposed by the authors [1] was usually around 17 kg higher than the latter, designed by the modified Vebe method [2,3] for 1 m^3 of concrete, for the same mix proportion [1].

Flexural strengths of conventional steel fibre reinforced concrete (SFRC) have been investigated since the 1980s [4–11]. A vast amount of literature deals with flexural strength, residual flexural strength, toughness, toughness indexes, crack development and propagation, fibre bridging law, fracture energy, and so on. Neocleous et al. [12,13] investigated the flexural performance of steel fibre-reinforced RCC for pavements, while the steel fibres were recovered from used tyres, whereas the mix was conventional RCC. Kagaya et al. [14] investigated the mix design method for steel fibre reinforced RCC pavements by employing the modified Proctor compaction method.

* Corresponding author. Tel.: +44 24 7765 8992.
E-mail address: john.karadelis@coventry.ac.uk (J.N. Karadelis).

http://dx.doi.org/10.1016/j.conbuildmat.2015.04.059
0950-0618/

It is seen that the mechanical properties of SFR–RC–PMCs have not been investigated to date. In addition, steel fibres in these types of mixes may exhibit a different behaviour to those in conventional SFRCs, due to the fact that the former contains much less cement paste than the conventional concrete, and roller compaction may result in deformation of steel fibres. Furthermore, the flexural performance of PVA (Polyvinyl Alcohol) modified concrete has rarely been investigated. Therefore, it is crucial to investigate the flexural performance of SFR–RC–PMC for overlay pavement design. This article aims to reveal the flexural performance, especially the equivalent flexural strengths of SFR–RC–PMC for overlay pavement design and the efficiency of fibres in RCC.

2. Mix proportion and specimen preparation

The ingredient materials used (apart from the 50 mm-long fibre) were presented in Ref. [1] in detail. The 50 mm-long fibre was the hooked-end type, with an aspect ratio of 80. The test beams of eight mixes are tabulated in Table 1. Two types of polymers, i.e. SBR (Styrene Butadiene Rubber) and PVA (Polyvinyl Alcohol) and two types of steel fibre, i.e. 35 mm-long and 50 mm-long were used. Super-plasticizer was added in the PVA modified concrete to reduce water content and obtain high strength, while the SBR modified concrete did not incorporate any admixtures. Among a total of eight mixes, five mixes, SBRPMC1%-35, SBRPMC1.5%-35, SBRPMC2%-35, PVAPMC1.5% and SBRPMC1.5%-50 (final numbers of mix ID indicate length of fibres), were SFR–RC–PMC, whose water contents were determined using the M-L compaction method [1]. Mix SBRPMC0%, did not contain fibre and was used as the matrix of mixes SBRPMC1.5%-35 and SBRPMC1.5%-50. Also, it was purposely used for the evaluation of the relative toughness of the same mixes. All beams of the six mixes were fabricated in steel moulds using the vibrating compactor shown in Fig. 1, which was purposely designed for specimen formation. The dimensions of the beams of the six mixes were 80 (W) × 100 (H) × 500 (L) mm.

The mixing procedure can be found in Ref. [1]. The mix compaction was carried out in two layers. Each layer was about 40–50 mm thick. The vibrating compaction lasted 30–50 s per layer for SBRPMC, and 60–90 s for PVAPMC until mortar formed a ring around the perimeter of the moulds. The surface of each layer was roughened before accepting the next layer of material. The specimens were de-moulded in twenty-four hours. The SBR modified concrete specimens were cured in water for five days whereas the PVA specimens for seven days, followed by air curing until the test day. The ages of the specimens for tests were 28–40 days.

The conventional SFRC, i.e. Con.SBRPMC1.5%-35, was intended for comparison with the mix SBRPMC1.5%-35 to reveal the efficiency of fibres. The former had the same ingredients and mix proportion as the latter except for the water content. The mix Con.SBRPMC0% acted as the matrix of mix Con.SBRPMC1.5%-35. The slump of the mix Con.SBRPMC1.5%-35 was 130 mm. The dimensions of the beams of both mixes were 100 (W) × 100 (H) × 500 (L) mm, fabricated in steel moulds on the vibrating table. The mixing and curing procedures of both mixes were the same as for mix SBRPMC1.5%-35.

The beam dimensions recommended by BS [15] are 150 (W) × 150 (H) × 550 (L) mm. The beams used in this study were 80 (W) × 100 (H) × 500 (L), recommended by ASTM [16]. The notches were saw cut to the specified depth by a circular saw one day prior to testing. The width of the notches was 3.5–4 mm, complying with BS [15].

3. Flexural strength of PMC beams

3.1. Strength under four-point bending (4PB) and three-point bending (3PB)

The representative test methods for steel fibre reinforced concrete currently available are the ASTM [16] and BS [15] methods. The intact beams of the three mixes, SBRPMC1.5%-35, PVAPMC1.5%-35 and Con.SBRPMC1.5%-35, were tested using four point bending (4PB) arrangements. The loading configuration and experimental setups are shown in Fig. 2(a) and (b). The test procedure complied with ASTM [16]. Two LVDTs measuring net deflection were mounted on both sides of the frame. A hydraulic servo-closed loop test facility with a maximum load capacity of 150 KN was used. The loading rate was controlled by a LVDT placed at mid-span. The representative mid-span deflection was the average of the two LVDT readings. The rate of increase of net deflection was 0.0017 mm/s until the LVDT reading reached 0.5 mm; after the 0.5 mm were reached the rate was increased to 0.0033 mm/s. This is within the range specified by ASTM [16]. The load and vertical displacements were continuously recorded at a frequency of 5 Hz. The maximum flexural strength, f_p, and the residual flexural strengths, $f_{R,0.5}$ and $f_{R,2}$ were calculated using Eq. (1) in accordance with ASTM [16]:

$$f_j = \frac{300P_j}{Bh^2} \tag{1}$$

where: $j = P$ (for peak), or $j = R,0.5$, or $j = R,2$.

In this case, R denotes residual flexural strength. P_p, is the maximum load. $P_{p,0.5}$ is the load corresponding to mid-span deflection equal to 0.5 mm. $P_{p,2}$, is the load corresponding to mid-span deflection equal to 2 mm. f_p, is the maximum flexural strength. $f_{R,0.5}$ and $f_{R,2}$ are strengths corresponding to mid-span deflections of 0.5 and 2 mm respectively. B and h are the breadth and depth of the beam.

The relationships of flexural strength vs. mid-span deflection for the three mixes are presented in Fig. 3. The mid-span deflection was recorded and averaged by two LVDT readings. The laboratory tests showed that all the SBRPMC1.5%-35 and PVAPMC1.5%-35 beams failed with multiple cracking under the 4PB test. However, for concrete used as an overlay on worn concrete pavements, a single reflective crack will initiate from the location of an underlying existing crack of the worn pavement. Therefore, the 3PB test arrangement was chosen as more suitable for concrete overlays.

The reason for the sharp drop of the flexural strength of mix PVAPMC1.5%-35 shown in Fig. 3 is due to the fact that it exhibited lower flexural toughness than the other two mixes. The flexural performance of the same mix under a 3PB test, shown in Fig. 4, shows also the same tendency. The mix contained 1.5%-35 mm length steel fibre by volume.

The three-point bending (3PB) test, recommended by BS [15], was employed to measure the flexural performance. The experimental setup is shown in Fig. 2(c) and (d). Six mixes shown in Fig. 4 were tested under 3PB complying with the BS [15]. The beams measured 80 (W) × 100 (H) × 500 (L) mm, spanning 400 mm with a mid-span notch of 20 mm depth. They were loaded at mid-span. It should be pointed out that the dimensions of the beams used in this study were different from those proposed by BS [15], which are 150 (W) × 150 (H) × 550 (L) mm, with span of 500 mm, centrally loaded and notched to the depth of 25 mm.

Table 1
Proportion of mixes with optimal water content determined by M-L method (Cem. = cement, Supe. = superplasticizer, Ad. water = added water).

Mix ID	Mix proportion							Fibre by volume (%)	Wet densi. (kg/m^3)
	Cem.	Aggr.	Sand	SBR	PVA	Supe.	Ad. water		
SBRPMC1%-35	1	1.266	1.266	0.217	0	0	0.072	1	2479
SBRPMC1.5%-35	1	1.266	1.266	0.217	0	0	0.095	1.50	2482
SBRPMC2%-35	1	1.266	1.266	0.217	0	0	0.103	2	2499
PVAPMC1.5%-35	1	1.266	1.266	0	0.02	0.025	0.228	1.50	2466
Con.SBRPMC1.5%-35	1	1.266	1.266	0.217	0	0	0.245	1.50	
SBRPMC1.5%-50	1	1.266	1.266	0.217	0	0	0.095	1.50	2482
Con.SBRPMC0%	1	1.266	1.266	0.217	0	0	0.245	0	
SBRPMC0%	1	1.266	1.266	0.217	0	0	0.095	0	

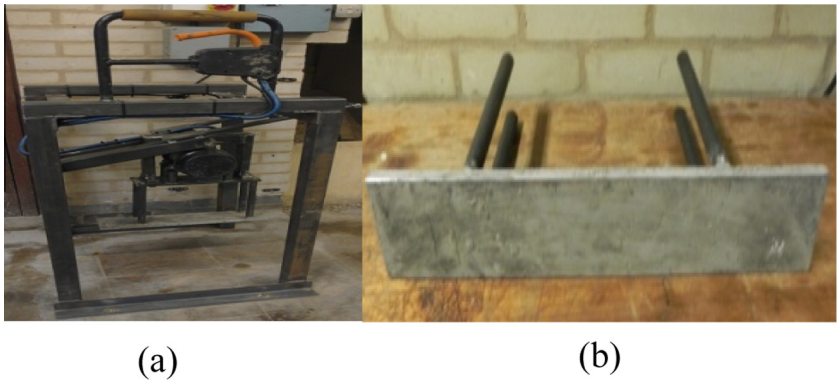

Fig. 1. (a) Vibrating compactor. (b) Steel plate for compaction.

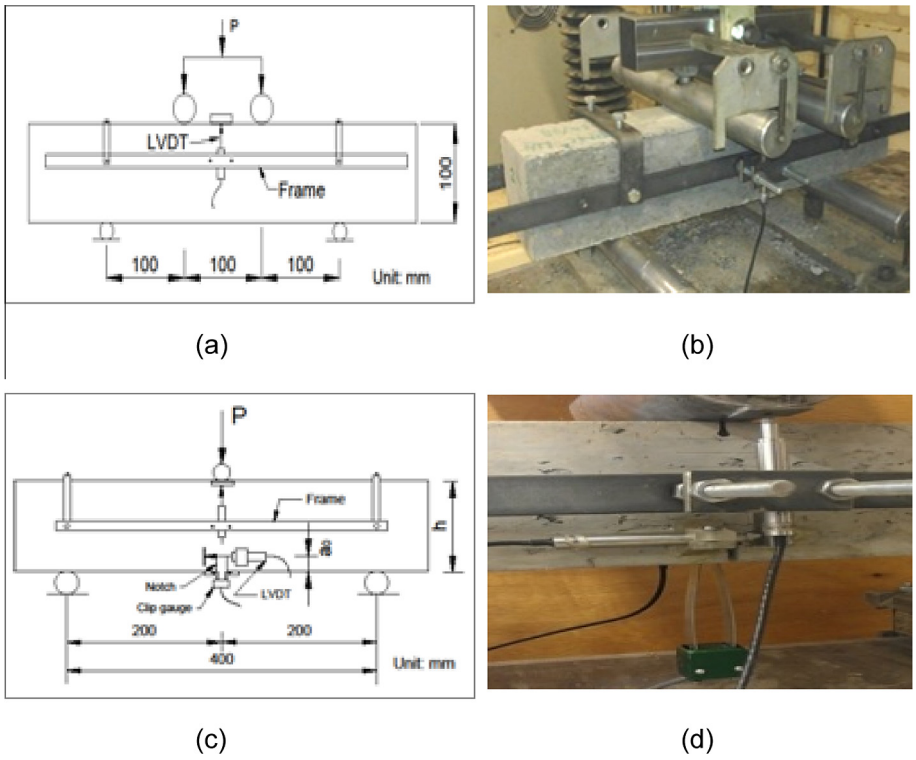

Fig. 2. (a) Un-notched beam under 4PB. (b) Experimental setup of 4PB test. (c) Notched beam under 3PB. (d) Close view of clip gauge and LVDTs mounted on the beam under 3PB.

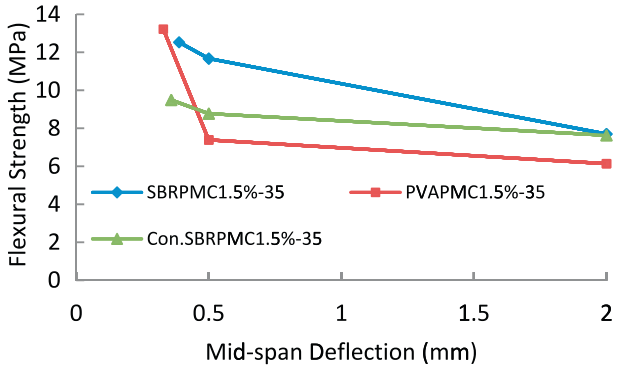

Fig. 3. Flexural strengths of un-notched beams for three different mixes under 4PB.

The loading machine was the same as the one used in the 4PB test. One LVDT was fixed on the frame for measuring mid-span (point-load) deflection. The other, for measuring notch tip opening displacement (CTOD), was secured on the beam surface, while the clip gauge was mounted on the underside to measure the crack mouth opening displacement (CMOD) and control the loading rate. Test data were automatically recorded by a computer at the frequency of 5 Hz. The loading rate procedure, controlled by CMOD, was as follows: 0.0001 mm/s until CMOD reached 0.2 mm; 0.0033 mm/s until CMOD reached 3 mm; then 0.005 mm/s until failure of the specimen. The rate of increase CMOD used was much lower than that proposed in the BS [15], which is 0.00083 mm/s until CMOD = 0.1 mm; after that 0.0033 mm/s. All tests were accurately controlled; no abrupt failures occurred and suitable load-CMOD, load-CTOD, and load–load point deflection curves were obtained. These results were used to evaluate the maximum flexural strength, residual flexural strength, equivalent flexural

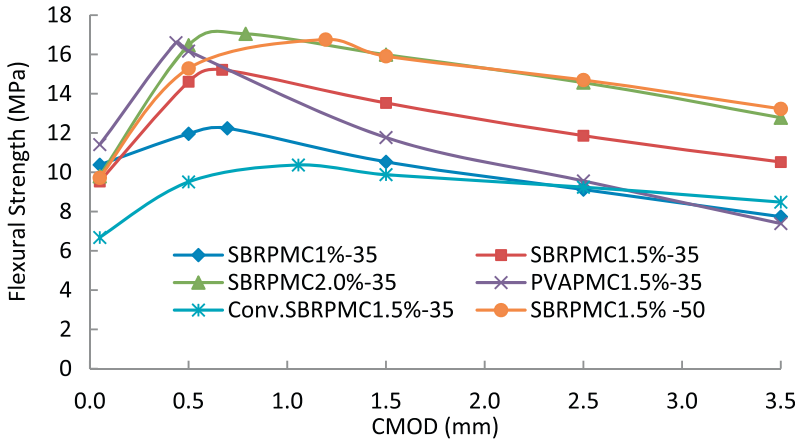

Fig. 4. Flexural strengths of six 20 mm-notched PMC beams under 3PB.

strength, relative toughness index, and total fracture energy and size effects.

The flexural strengths were evaluated according to BS [15], using Eqs. (2)–(4):

$$f^{f}_{ct,L} = \frac{3SP_L}{2Bh^2_{sp}} \tag{2}$$

$$f_{R,j} = \frac{3SP_j}{2Bh^2_{sp}} \tag{3}$$

$$f_p = \frac{3SP_P}{2Bh^2_{sp}} \tag{4}$$

Where: $f^{f}_{ct,L}$ is the limit of proportionality (LOP) in MPa. P_L is the load corresponding to LOP (N). S is the span (mm). B is the breadth (width) of the specimen (mm). h is the depth (height) of the beam (mm). a_0 is the depth of notch (mm). h_{sp} is the distance between the tip of the notch and the top of the specimen (mm). $f_{R,j}$ is the residual flexural tensile strength. CMOD = j, j = 0.5, 1.5, 2.5, and 3.5 mm, respectively. P_j is the load corresponding to CMOD = j, (N); f_p is the maximum flexural tensile strength (MPa). P_P is the peak load (N).

The flexural strength–CMOD relationships are plotted in Fig. 4. The compressive strengths of blocks saw-cut from the tested beams are listed in Table 2, while the interfacial fracture toughness and splitting tensile bond strength of composite specimens are shown in Table 3. The details for testing interfacial fracture toughness can be found in Ref. [17]. It is seen that:

(a) Compared to conventional SFRC, SFR–RC–PMC exhibited very high flexural strengths, which are desired for worn concrete pavement rehabilitation;

(b) Compared to the strengths measured under 4PB for the same mix, the obtained strengths under 3PB are remarkably higher.

However, the flexural strengths cannot be directly used for overlay pavement design. The design method for SFRC pavements proposed by Altoubat et al. [18], requires the flexural strengths to be converted into equivalent flexural strengths.

3.2. Size effect on flexural strength

There are two major approaches to explaining the effect of size on the strength of a material: the statistical and deterministic approaches. A representative statistical approach is Weibull's theory [19], while the classic deterministic approach is by Bazant [20,21], based on fracture mechanics. According to Weibull's theory [19], a larger specimen has a weaker strength because it has a higher probability of having larger and more severe flaws or defects in it.

Table 4, Figs. 3 and 4 indicate that for the same mix, the measured flexural strength under 4PB is higher than that under 3PB. The reason for this can be explained by Weibull's theory. As has been presented earlier, the tested beams in this study were of dimensions 80 (W) × 100 (H) × 400 (S) mm. The beams for 3PB were saw-cut a central notch of 20 mm prior to testing, while the beams for 4PB were intact. In order to use the equivalent concept (presented later), proposed by the Japan Society of Civil Engineers (JSCE-SF4) [22], the flexural strength obtained using 3PB test has to be converted to that by 4PB test.

It is seen from Fig. 4 that the flexural strength-CMOD curves for all mixes are basically parallel to each other except for the mix

Table 2
Compressive strengths of blocks saw-cut from tested beams.

Mix ID	Num. of block	Compres. strength (MPa)	
		Average	STDEV
SBRPMC 1%-35	3	83.91	6.69
SBRPMC 1.5%-35	4	79.61	1.48
SBRPMC 2%-35	3	84.76	0.27
Con.SBRPMC 1.5%-35	8	68.18	2.82
PVAPMC 1.5%-35	6	105.87	3.78

Table 3
Mechanical properties of interface of SBRPMC1.5%-35, PVAPMC1.5%-35 and OPCC to OPCC composite specimens.

Interfacial fracture toughness (J/m^2)	SBRPMC1.5%-35 on-OPCC	Roughened interface	52.0
		Smooth interface	22.6
Splitting tensile bond strength (MPa)	SBRPMC1.5%-35 on-OPCC	Roughened interface	2.96
		Smooth interface	1.8
	PVAPMC1.5%-35 on-OPCC	Roughened interface	3.7
	OPCC-on-OPCC	Roughened interface	2.68

Table 4
Calculation of standard equivalent flexural strength $f_{e,3}$.

Mix ID	$f_{e,5}$ (MPa)	f_p in 3PB (MPa)	f_p in 4PB (MPa)	First convers. factor β_1	Second convers. factor β_2	$f_{e,3}$ (MPa)
SBRPMC1%-35	8.87	12.24	N/A	0.823	0.813	5.93
SBRPMC1.5%-35	10.86	15.22	12.53	0.823	0.813	7.27
SBRPMC2%-35	14.05	17.05	N/A	0.823	0.813	9.4
Con.SBRPMC1.5%-35	9.13	10.37	9.49	0.915	0.813	6.79
SBRPMC1.5%-50	14.24	16.76	N/A	0.823	0.813	9.53
PVAPMC1.5%-35	10.05	16.6	13.2	0.795	0.813	6.49

PVAPMC1.5%-35. This indicates that all mixes have the same scale factor for equivalent strength conversion. The conversion factor (β_1) can be taken as the ratio of maximum flexural strength under 3PB to that under 4PB. It is used for converting the strength of the small volume to the large volume, which can be explained by Weibull's theory [19].

The maximum flexural strengths tested under the 3PB and 4PB are listed in Table 4. The conversion factor, β_1 can be easily obtained by simply comparing the f_p in the 4PB to the 3PB, using Eq. (5). The calculated β_1 is listed in Table 4.

$$\beta_1 = \frac{f_p(\text{in 4PB})}{f_p(\text{in 3PB})} \tag{5}$$

In this study [23], the flexural strength affected by the height of beams was experimentally investigated. For this purpose, the SBRPMC1.5%-35 beams with the dimensions of 80 (W) × 100 (H) × 400 (S) mm and 100 (W) × 150 (H) × 500 (S) mm and with different notch lengths, were tested under 3PB to investigate the size effect on maximum flexural strengths. The size effect law proposed by Bazant [21] was employed. The splitting tensile strength taken from three cylinders with the dimensions Φ100 × 170 mm was 9.88 MPa. Consequently, the size effect law obtained using regression analysis for maximum flexural strength of mix SBRPMC1.5%-35 is [23]:

$$f_p = \frac{80.42}{\sqrt{\frac{h_{sp}}{2.7} - 1}} \tag{6}$$

where: f_p is the maximum flexural strength (MPa). h_{sp} is as per Eqs. (3) and (4).

Eq. (6) will be used to determine the standard equivalent flexural strength later.

3.3. Equivalent flexural strength

Altoubat et al. [18] tested an actual size SFRC slab on an elastic foundation, and related the load carrying capacity to the equivalent flexural strength proposed by the Japan Society of Civil Engineers (JSCE-SF4) [22]. He then proposed a simple design method for SFRC pavements. The equivalent flexural strength, $f_{e,3}$ proposed by JSCE-SF4 [22] was measured by conducting a 4PB test. The test beam was 150 (W) × 150 (H) × 450 (S) mm. The equivalent flexural strength was calculated using the area enveloped by load-central deflection curve, and is evaluated by Eq. (7).

$$f_{e,3} = \frac{S.A_{3\text{mm}}}{2Bh^2} \tag{7}$$

where: $A_{3\text{mm}}$ is the ratio of the area enveloped under the load-midspan deflection curve, from the origin to the load at deflection equal to 3 mm. S is the span. B and h are the breadth (width) and height of beam, respectively.

However, the beams used in this study were centrally notched, had dimensions of 80 (W) × 100 (H) × 400 (S) mm and were tested under the 3PB. In order to use the equivalent flexural strength concept, which is defined at the specified deflection of 3 mm, it is necessary to correlate the two different test methods via the relationship between deflection and CMOD.

In the post-peak region of a 3PB test, a hinge forms at the top of the beam, hence the residual flexural strength is only dependent on the fibre reactions. For different dimensional beams under bending test, the fibre effect can be regarded as similar if the crack lengths and crack opening displacements of the two beams are identical. In order to compare the residual strengths in the post-peak region measured from different geometrical beams, Giaccio et al. [24] proposed an approach to determine the deflection limits of small beams to obtain design parameters of fibre-reinforced concrete.

Consider the two types of beams with different dimensions under 4PB and 3PB shown in Fig. 5. Beam one is the standard un-notched beam with the dimensions S_1 and h_1 under 4PB, while beam two is a centrally-notched beam with dimensions S_2 and h_2 and initial notch a_0 under 3PB. In order to obtain identical fibre bridging effect, CMOD_1 should be equal to CTOD_2.

In the post-peak region, the relationships between deflection and the rotation angle and crack opening is as follows:

$$\delta_1 = \theta_1 s_1/2 \tag{8}$$

$$\delta_2 = \theta_2 s_2/2 \tag{9}$$

$$\text{CMOD}_1 = 2h_1\theta_1 \tag{10}$$

$$\text{CTOD}_2 = 2(h_2 - a_0)\theta_2 \tag{11}$$

From the equations above and the condition of $\text{CMOD}_1 = \text{CTOD}_2$, the following equation is obtained:

$$\frac{\delta_1}{\delta_2} = \frac{s_1(h_2 - a_0)}{s_2 h_1} \tag{12}$$

The standard beam for testing equivalent flexural strength is 150 (W) × 150 (H) × 450 (S) mm, and the specified deflection, δ_1 = 3 mm. The beams used in this study were 80 (W) × 100 (H) × 400 (S) mm with an initial notch of 20 mm. Hence, substitution of these dimensions into Eq. (12) results in:

$$\delta_2 = 1.67\delta_1 \tag{13}$$

Thus, the corresponding deflection limit, δ_2, determined using Eq. (13) is 5 mm. Hereafter, the equivalent strength for the deflection limit of 5 mm is denoted as $f_{e,5}$. The equivalent flexural strengths $f_{e,5}$ are listed in Table 4.

3.4. Standard equivalent flexural strength, $f_{e,3}$

However, the equivalent flexural strength, $f_{e,5}$, cannot be used directly for the design of the SFRC overlay pavement proposed by Altoubat et al. [18], because specimen sizes affect the flexural strength significantly. As has been presented earlier, the tested beams in this study were of dimensions 80 (W) × 100 (H) × 400 (S) mm with a central notch of 20 mm, quite different from the standard beam for testing equivalent flexural strength proposed by JSCE-SF4 [22], which is of the dimensions 150 (W) × 150 (H) × 450 (S) mm. Therefore, the $f_{e,5}$ above needs to be converted by taking the size effect into account.

It is seen from Fig. 4 that the flexural strength-CMOD curves for all mixes are basically parallel to each other except for the mix PVAPMC1.5%-35. This indicates that all mixes have the same scale factor for equivalent strength conversion. In order to use the SFRC pavement design method proposed by Altoubat et al. [18], the $f_{e,5}$ has to be converted twice to obtain the standard equivalent flexural strength, $f_{e,3}$.

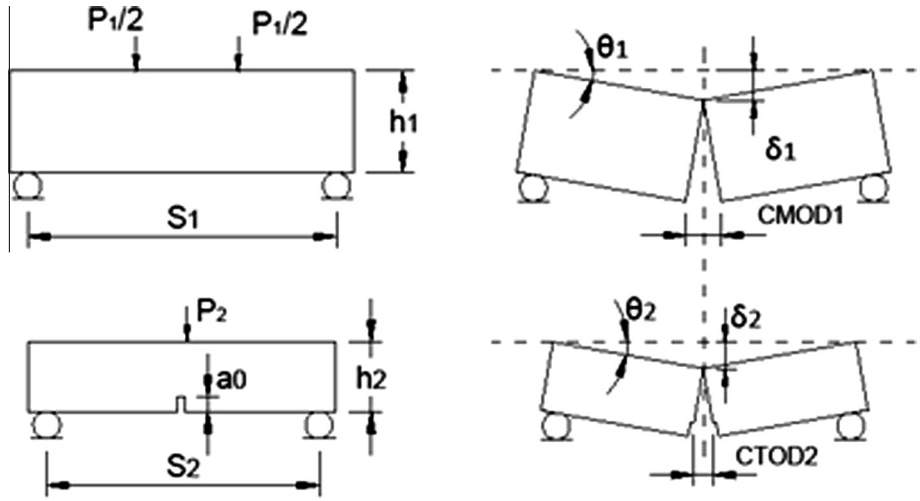

Fig. 5. Correlation of δ_1 and δ_2 of two beams with different dimensions.

First, it has to be converted from the 3PB to 4PB. Its conversion factor (β_1) has been determined previously. Second, it has to be converted from a 4PB test with the beam of 100 mm height to a 4PB test with the standard beam of 150 mm height, via the conversion factor (β_2) that can be determined using the size effect equation (6) for mix SBRPMC1.5%-35.

Both conversion factors are attributed to the size effect. Factor β_2 is for converting the strength of the 'short' beam to that of the 'tall' beam, explained thoroughly by Bazant's theory [21].

The second conversion factor, β_2, is calculated in the following way:

$$\beta_2 = \frac{f_p(\text{in150 mm} - \text{height beam})}{f_p(\text{in100 mm} - \text{height beam})} = \frac{\sqrt{\frac{100}{2.7} - 1}}{\sqrt{\frac{150}{2.7} - 1}} = 0.813 \quad (14)$$

$$\beta = \beta_1 \cdot \beta_2 \quad (15)$$

The process of calculating the total conversion factor β and the standard equivalent flexural strength, $f_{e,3}$, are tabulated in Table 4. It is seen from Table 4 that the mix PVAPMC1.5%-35 developed the lowest standard equivalent flexural strength, although it exhibited very high maximum flexural strength. The standard equivalent flexural strength, $f_{e,3}$ can be used for SFR–RC–PMC overlay pavement design.

3.5. Verification

The experimental results of SBRPMC1.5%-35 beams with different notch lengths and beam depths, which were previously used for establishing the size effect law, were reanalysed to verify the method for calculating the equivalent flexural strength, $f_{e,3}$, which should be theoretically identical. Two types of beams, i.e. three 80 (W) × 100 (H) × 400 (S) mm with 40 mm-long notch and two 100 (W) × 150 (H) × 500 (S) mm beams with 25 mm-long notch were analysed. The deflection limit for the former, determined using Eq. (11), was 6.8 mm, while that of the latter was 4 mm. The equivalent flexural strengths $f_{e,5}$, $f_{e,6.8}$ and $f_{e,4}$ corresponding to the deflection limits of 5, 6.8 and 4 mm, and their conversion factors are tabulated in Table 5. It is seen that the standard equivalent flexural strengths, $f_{e,3}$, determined using the method proposed are approximately identical. This validates the method for calculating the standard equivalent flexural strength, $f_{e,3}$, for overlay pavement design.

4. Efficiency of steel fibre in roller–compacted concrete

Compared to conventional SFRCs, the SFR–RC–PMC has more air voids and relatively less cement paste (Table 6), hence this may lead to:

(a) The steel fibres may not be fully bonded by cement paste;
(b) The steel fibres may be deformed during specimen formation due to compaction by the vibrating compactor.

The two factors may consequently lead to poor steel fibre efficiency. In addition, the efficiency of 50 mm-long fibres also need to be quantitatively investigated by comparison with 35 mm-long fibres. Steel fibres have been successfully used in conventional concrete to improve the performance of concrete for several decades. The conventional concrete containing the same steel fibre type and fibre content, can be a reliable benchmark for the investigation of the fibre efficiency in SFR–RC–SBRPMC.

Table 6 shows the main physical parameters of the three mixes SBRPMC1.5%-35, SBRPMC1.5%-50 and Con.SBRPMC1.5%-35. The mix Con.SBRPMC1.5%-35 was conventional concrete, its slump of fresh mix was measured to be 130 mm. The three mixes contained the same fibre content and the beams were of the same dimensions to avoid any size effect.

Table 6 clearly indicates that the water to cement ratios and cement paste contents of mixes SBRPMC1.5%-35 and SBRPMC1.5%-50 are much lower than those of the conventional Con.SBRPMC1.5%-35. Also, the former have higher air content than the latter.

Table 5
Standard equivalent flexural strength determined using experimental results of beams with different notch length and beam depth (a_0 = notch length, h = height of beam).

Mix ID	a_0/h (mm/mm)	$f_{e,5}/f_{e,6.8}/f_{e,4}$ (MPa)	f_p in 3PB (MPa)	f_p in 4PB (MPa)	β_1	β_2	$f_{e,3}$ (MPa)
SBRPMC1.5%-35	20/100	10.86	15.22	12.53	0.823	0.813	7.27
	40/100	13.31	16.85	12.53	0.743	0.813	8.04
	25/150	8.89	11.94	N/A	0.823	1.00	7.32

Table 6
Comparison of physical properties of five mixes.

Mix ID	Workability of fresh mixes	W/C	Cem. paste by volume (%)	Air content (%)
SBRPMC1.5%-35	Dry, non-slump	0.206	37.94	2.94
SBRPMC1.5%-50	Dry, non-slump	0.206	37.94	2.94
Con.SBRPMC1.5%-35	Wet, slump of 130 mm	0.355	42.3	1.2
SBRPMC0%	Dry, non-slump	0.206	N/A	N/A
Con.SBRPMC0%	Wet, slump > 130 mm	0.355	N/A	N/A

Note: the water for determining water to cement ratio and cement paste fraction included also the water contained in SBR but excluded the water absorbed by the coarse aggregate.

Table 7
Comparison of macro-mechanical properties of three mixes.

Mix ID	f_p (MPa)	$f_{e,3}$ (MPa)	G_F (J/m^2)	I_t
SBRPMC1.5%-35	15.22	7.27	18,580	221
SBRPMC1.5%-50	16.76	9.53	28,300	337
Con.SBRPMC1.5%-35	10.37	6.79	15,650	103

Table 8
Fibre bridging law for stage-II under 3BP [units: σ (MPa), and w (mm)].

Mix ID	Fibre bridging law for stage-II under flexure
SBRPMC1.5%-35	$\sigma_{II}(w) = -0.0056w^3 + 0.1612w^2 - 1.5044w + 5.9306$ $0.958 \leqslant w \leqslant 12.45$
Con.SBRPMC1.5%-35	$\sigma_{II}(w) = 0.0012w^3 - 0.025w^2 - 0.0461w + 2.4392$ $0.907 \leqslant w \leqslant 12.64$
SBRPMC1.5%-50	$\sigma_{II}(w) = -0.0012w^3 + 0.0654w^2 - 0.9482w + 5.9164$ $1.063 \leqslant w \leqslant 12.99$

The beam dimensions and test procedures for the three mixes SBRPMC1.5%-35, SBRPMC1.5%-50 and Con.SBRPMC1.5%-35 have been presented in Sections 2 and 3.1. The three mixes were tested under 3PB, and the experimental data have been analysed to evaluate maximum flexural strength, f_p, equivalent flexural strength, $f_{e,3}$, relative toughness index, I_t, defined as the ratio of fracture energy of SFRC to that of unreinforced concrete [27] and total fracture energy, G_F [23]. These mechanical parameters are rearranged to study the fibre efficiency in the following:

The total fracture energy was evaluated using the method recommended by the RILEM code [25], i.e. it is equal to the work done by the externally applied load divided by the area of fractured section of the beam.

The beams of mixes SBRPMC0% and Con.SBRPMC0% had mid-span saw-cut notches to the depth of 33 mm made prior to the test. The 3PB test was conducted to measure fracture energy. The specimen dimensions and test procedure complied with the code of RILEM Report 5 1991 [26]. However, the much lower than the recommended by the same code CMOD - control loading rate was 0.0001 mm/s, in an effort to obtain stable load–deflection curves. The test for each beam lasted about 30 min, longer than that recommended by the RILEM code [26]. It is seen from Table 7 that:

(a) The fibre in mix SBRPMC1.5%-35 exhibited much higher efficiency than the mix Con.SBRPMC1.5%-35, indicating that the efficiency of fibres in these mixes is much higher than that in conventional concrete.
(b) The efficiency of fibres with aspect ratio of 80 in mix SBRPMC1.5%-50 was much higher than the fibres with aspect ratio of 60 in SBRPMC1.5%-35, indicating the fibre aspect ratio has remarkable influence on the flexural performance.

5. Mechanism of fibre efficiency

Observations on SFRC beam under 3PB test indicated that the crack initiated from the notch tip, and extended monotonically with load increments. The crack continued to extend but the applied load begun to fall after the peak load was reached and a hinge formed beneath the top of the beam. The complete process of failure of SFRC beam in flexure consisted of two stages: At stage I, prior to hinge formation, the flexural performance mainly depends on the interaction of matrix and fibres. At stage II, after the hinge formation, the flexural behaviour depends mainly on the resistance induced by fibre traction. Therefore, it is reasonable to use the relationship of fibre tensile stress and crack face opening displacement (fibre bridging law) at stage-II to reveal the reasons why the efficiency of fibre in RCC was much higher than that in conventional concrete. The fibre bridging at stage-II serves also as the fibre pull-out test. Table 8 presents the fibre bridging law, for stage-II, for three mixes, established by using inverse analysis presented in Ref. [28] in detail. Fig. 6(b) provides a graphical representation of the law for the same three mixes.

It is seen from Fig. 6(b) that both mixes SBRPMC1.5%-35 and Con.SBRPMC1.5%-35 contained the same amount and type of fibre, however the former exhibited higher tensile strength than the latter, for a given face opening displacement. It is clear that the main mechanism for the RCC having higher fibre efficiency than conventional concrete is attributed to a lower water to cement ratio, resulting in higher friction between fibre and mortar, although the air content of the former was higher than the latter. In addition,

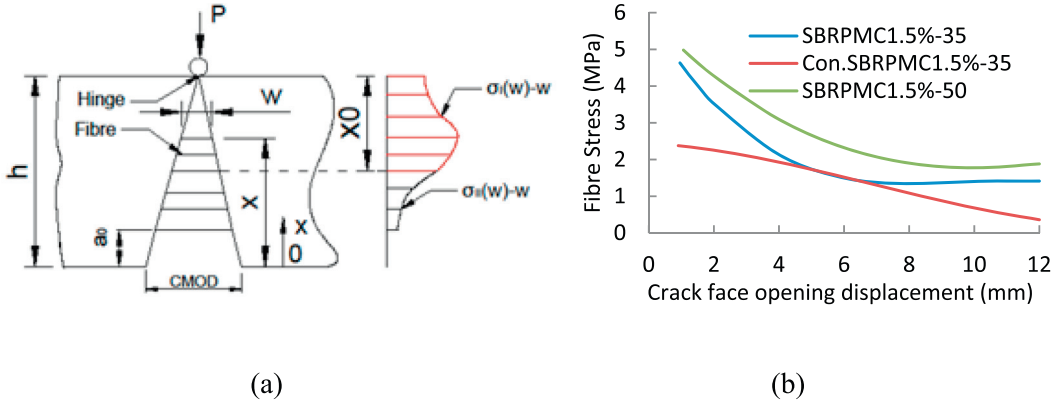

Fig. 6. (a) Fibre tensile stress after a hinge formation beneath the point load (a_0 = notch depth). (b) Plots of fibre bridging laws in polynomial form as listed in Table 8.

the curve of fibre bridging law of SBRPMC1.5%-50 is above the curve of SBRPMC1.5%-35 at all crack face opening displacements, implying that the former provided higher fibre traction.

The fibre bridging law can serve as an index to evaluate the fibre efficiency for the selection of ingredients during the mix design process in practical (site) applications. For example, mixes SBRPMC1.5%-35 and SBRPMC1.5%-50, in Table 8, are the same (have identical proportions of ingredients), only the former incorporates shorter fibres than the latter. It is apparent from Fig. 6(b) that SBRPMC1.5%-50 is more efficient than SBRPMC1.5%-35 because the fibres of mix -50 provide higher tensile strength than those of -35, for the same crack opening displacement. In this case, the fibre bridging law specified in Table 8, can be used to predict the flexural performance of beams made of the three different mixes.

6. Concluding remarks

(1) Compared to conventional steel fibre-reinforced concrete, steel fibre-reinforced roller-compacted polymer modified concrete developed very high flexural strength. This is very favourable to worn concrete pavement rehabilitation.
(2) The standard equivalent flexural strengths evaluated using the method proposed by this study are listed in Table 4, and can be directly used for overlay pavement design. The method, using the identical fibre bridging concept and size effect, has been verified successfully.
(3) Mix SBRPMC1.5%-35 is deemed to be optimum for both, strength and workability. Mix PVAPMC1.5%-35 exhibited higher flexural and bond strength with the old concrete than mix SBRPMC1.5%-35 but unfortunately low equivalent flexural strength which is the basis of overlay design and thus is not a suitable mix for worn concrete pavement rehabilitation.
(4) The fibres in SFR–RC–PMC exhibited much higher efficiency than in conventional SFRC (consolidated by vibrating table). This is mainly attributed to a lower water to cement ratio. This indicates that these mixes are economically viable.

Acknowledgements

The financial support of the Engineering and Physical Sciences Research Council (EPSRC, Ind. Case Studentship, No. 08002550), and Aggregate Industries, UK, is gratefully acknowledged. The authors would like to express their gratitude to their colleague, Ms. Yi Xu, for her help during lab work; and to Mr. Ian Breakwell, senior technician at the Civil Engineering Laboratories, Coventry University for his valuable suggestions, comments and help. Special mention should also be made of Tarmac, AGS Mineraux, Power Minerals and Nippon Gohsei EU for providing materials for research.

References

[1] Lin Y, Karadelis JN, Xu Y. A new mix design method for steel fibre-reinforced, roller compacted and polymer modified bonded concrete overlays. Constr Build Mater 2013;48:333–41.
[2] ASTM C 1170-06. Standard test method for determining consistency and density of roller-compacted concrete using a vibrating table, ASTM Committee C09; 2006, USA.
[3] ACI Committee 207. Roller-Compacted Mass Concrete (ACI 207.5R-99), USA: ACI; 1999.
[4] Jenq YS, Shah SP. Crack propagation in fibre-reinforced concrete. J Struct Eng 1986;112(1):19–34.
[5] Gopalaratnam VS, Shah SP, Batson GB, Criswell ME, Ramakrishnan V, Wecharatana M. Fracture toughness of fibre reinforced concrete. ACI Mater J 1991;88(4):339–53.
[6] Banthia N, Trottier JF. Test method for flexural toughness characterization of fibre reinforced concrete: some concerns and a proposition. ACI Mater J 1995;92(1):48–57.
[7] Banthia N, Trottier JF. Concrete reinforced with deformed steel fibres. Part II: toughness characterization. ACI Mater J 1995;92(2):146–54.
[8] Armelin HS, Banthia N. Predicting the flexural post-cracking performance of steel fibre reinforced concrete from the pullout of single fibres. ACI Mater J 1997;94(1):18–31.
[9] Lok TS, Pei JS. Flexural behaviour of steel fibre reinforced concrete. J Mater Civ Eng 1998;10(2):86–97.
[10] Jeng F, Lin ML, Yuan SC. Performance of toughness indices for steel fibre reinforced shotcrete. Tunn Undergr Space Technol 2002;17:69–82.
[11] Denneman E, Wu R, Kearsley EP, Visser AT. Discrete fracture in high performance fibre reinforced concrete materials. Eng Fract Mech 2011;78:2235–45.
[12] Neocleous K, Angelakopoulos H, Pilakoutas K, Guadagnini M. Fibre-reinforced roller-compacted concrete transport pavements. In: Proceedings of the Institution of Civil Engineers, UK, Transport 164, May 2011 Issue TR2, 97–109.
[13] Neocleous K, Tlemat H, Pilakoutas K. Design issues for concrete reinforced with steel fibres, including fibres recovered from used tires. J Mater Civ Eng 2006;18(5):677–85.
[14] Kagaya M, Suzuki T, Kokubun S, Tokuda H. A study on mix proportions and properties of steel fibre reinforced roller-compacted concrete for pavements, (Translation from Proceedings of JSCE, No. 669/V-50, February 2001); 2001.
[15] British Standard BS EN14651:2005+A1. Test method for metallic fibre concrete – measuring the flexural tensile strength (limit of proportionality (LOP), residual), British Standard Institution, UK; 2007.
[16] ASTM C 1609/C 1609M-06 Standard Test Method for Flexural Performance of Fibre-Reinforced Concrete (Using Beam with Three-Point Loading). USA: ASTM International; 2006.
[17] Lin Y, Karadelis JN. Strain energy release rate at interface of concrete overlay pavements. Int J Pavement Eng 2014 [under review].
[18] Altoubat SA, Roesler JR, Lange DA, Rieder KA. Simplified method for concrete pavement design with discrete structural fibres. Constr Build Mater 2008;22:384–93.
[19] Quinn GD. Weibull strength scaling for standardized rectangular flexure specimens. J Am Ceram Soc 2003;86:508–10.
[20] Bazant ZP. Size effect in blunt fracture: concrete, rock, metal. J Eng Mech 1984;81(5):456–68.
[21] Bazant ZP. Fracture energy of heterogeneous materials and similitude in Fracture of Concrete and Rock. In: Shah SP, Swartz SE, editors. New York: Springer-Verlag; 1989, p. 229–241.
[22] Japan Society of Civil Engineers JSCE-SF4. Methods of tests for flexural strength and flexural toughness of steel fibre reinforced concrete, Concrete Library International, Part III-2, No. 3; 1984, p. 58–61.
[23] Lin Y. Optimum design for sustainable 'Green' bonded concrete overlays: controlling flexural failure [PhD Thesis]. UK: Department of Civil Engineering, Architecture and Building, Faculty of Engineering and Computing, Coventry University; 2014. [unpublished].
[24] Giaccio G, Tobes JM, Zerbino R. Use of small beams to obtain design parameters of fibre reinforced concrete. Cement Concr Compos 2008;30(4):297–306.
[25] RILEM, Committee on Fracture mechanics of concrete. Test methods: determination of the fracture energy of mortar and concrete by means of three-point bend test on notched beams, Mater Struct 1985;10(106):285–290.
[26] RILEM, Fracture mechanics test method for concrete, Report 5, 89-FMT. In: Shah SP, Carpinteri A, editors; 1991.
[27] ACI Committee 544.2R-89, Reapproved in 2009, Measurement of properties of fibre-reinforced concrete; 1988.
[28] Lin Y, Karadelis JN. On establishing the fibre bridging law by an inverse analysis approach. ASCE J Mater Civil Eng 2014 [under review].